Electrospun fibres from polyvinyl alcohol, poly(styrene sulphonic acid-*co*-maleic acid), and imidazole for proton exchange membranes

Romklaw Boonpoo-nga[a]**, Manus Sriring**[a]**, Pitak Nasomjai**[a]**, Surangkhana Martwiset**[b,c,*]

[a] Department of Chemistry, Faculty of Science, Khon Kaen University, Khon Kaen 40002 Thailand
[b] Materials Chemistry Research Centre, Department of Chemistry and Centre of Excellence for Innovation in Chemistry, Faculty of Science, Khon Kaen University, Khon Kaen 40002 Thailand
[c] Nanotec-KKU Centre of Excellence on Advanced Nanomaterials for Energy Production and Storage, Khon Kaen 40002 Thailand

*Corresponding author, e-mail: surama@kku.ac.th

ABSTRACT: Electrospun fibres from polyvinyl alcohol (PVA), poly(styrene sulphonic acid-*co*-maleic acid) (PSSA-MA), and imidazole for potential use as proton conducting membranes at elevated temperatures were prepared and characterized. The effect of PSSA-MA content (9, 17, 25, 33, 42, and 50% by weight of PVA) on solution properties was investigated. Fibre mats were obtained from solutions with 9–33% PSSA-MA. Solution viscosity increased with increasing PSSA-MA until reaching a maximum at 33% PSSA-MA. The effect of PSSA-MA content on fibre size and morphology was studied using scanning electron microscopy. Fibre diameter was found to increase with increasing solution viscosity. A solution with 25% PSSA-MA provided uniform and bead-free fibres with an average diameter of 485 nm. Thermal crosslinking of electrospun fibres was confirmed by attenuated total reflection Fourier transform infrared spectroscopy and thermogravimetric analysis. Electrospun fibres were thermally stable up to 250 °C. Fibres containing 25% PSSA-MA had a proton conductivity in non-humidified conditions comparable to that of a solvent-cast membrane with the same composition. The proton conductivity of a solvent-cast membrane was slightly higher than that of fibres over the temperature range studied.

KEYWORDS: conducting polymers, electrospinning, fuel cells, polyelectrolytes

INTRODUCTION

During the last decade, as a result of the decrease of fossil fuels and the increase of emission of greenhouse gases, many investigations for alternative environmental friendly fuel and energy sources have been conducted. Promising energy sources for vehicle and portable electronic devices are polymer electrolyte membrane fuel cells (PEMFCs) and direct methanol fuel cells (DMFCs). Among acid polymers serving as electrolytes in PEMFCs and DMFCs, Nafion, a perfluorosulphonated membrane with a fluorocarbon backbone and sulphonic acid pendants, is the most commercially successful membrane. Its use, however, is limited by high cost, high methanol permeability, and a decrease in proton conductivity at high temperatures and low humidity[1–3].

Reduction of methanol crossover through polymer electrolyte membranes (PEMs) can be achieved by either rational selection of membrane materials or manipulation of membrane morphology[4,5]. In the field of membrane pervaporation for dehydration of alcohols, many hydrophilic polymers such as polyvinyl alcohol (PVA) have been used because they preferentially permeate water and retain alcohol[6,7]. Although high water uptake facilitates proton conduction, an excessive water swelling leads to low mechanical strength in PEMs. To overcome the swelling problem in PVA-based membranes, the membranes are either crosslinked or incorporated with inorganic materials[8–10].

The development and the commercialization of perfluorosulphonic acid membranes are limited to operating temperatures below 100 °C because the proton transport mechanism, namely vehicular mechanism, relies on the presence of water[11,12]. Operation at higher temperatures offers many advantages including the increase in fuel cell efficiency[13], decrease in required platinum catalyst loading[14], improvement in CO tolerance[15], and simpler heat management. Amphoteric nitrogen-based heterocycles, such as imidazole, pyrazole, and benzimidazole, were shown to have intrinsic conductivity[16,17]. The use of these heterocycles as proton solvents provided comparable proton

conductivities to that of hydrated polymers [18, 19].

Electrospinning is a simple method to produce fibrous materials with diameters ranging from nanometres to micrometres. In recent report, Tamura and Kawakami demonstrated that upon an introduction of nanofibres, membrane stability was improved, and gas permeability can be controlled [20]. Electrospinning of Nafion solution was challenging due to aggregation of ionic groups [21]; however, with an addition of PVA, sprayable solutions were produced [22]. Our group also reported the successful preparation of electrospun fibres of poly(styrene sulphonic acid) (PSSA) and PVA. The water stability of the fibres was improved by heat-treatment at 120 °C [23].

In this work, electrospun fibres of PVA, poly(styrene sulphonic acid-*co*-maleic acid) (PSSA-MA), and imidazole were prepared and characterized. PSSA-MA was chosen as proton source because of its low cost and relative high proton conductivity. PVA would enhance the spinnability of PSSA-MA into fibres, and provide hydrophilic properties, high density of hydroxyl groups for crosslinking reaction and excellent methanol barrier. Imidazole was employed as proton solvent. The effect of PSSA-MA content on solution properties, shape, and size of the fibres was studied. Surface morphology was characterized using scanning electron microscopy. Thermal properties of fibres were also investigated. Proton conductivity of fibres was measured using impedance spectroscopy in non-humidified condition, and the result was compared with that of solvent-cast membrane with the same PSSA-MA content.

MATERIALS AND METHODS

Materials

Poly(vinyl alcohol) (PVA, 95% hydrolysed, average MW 95 000) was purchased from Acros Organics. Poly(4-styrenesulphonic acid-*co*-maleic acid) (PSSA-MA, SSA:MA = 3:1, MW 20 000), and imidazole (99%) were purchased from Sigma-Aldrich. All chemicals were used as received.

Characterization

Surface morphology was studied using a scanning electron microscope (LEO 1450VP, UK). The average diameter of the fibres was determined by analysing 200 fibres in micrograph using WCIF ImageJ program. The viscosities of polymer solutions were measured at room temperature at a speed of 20 rpm using a digital viscometer (Brookfield, model DV-II). The reported values were the means of three measurements. Fourier transform infrared (FTIR) spec-
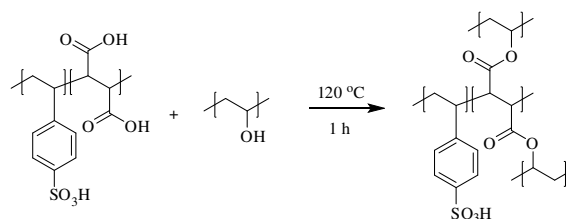
Fig. 1 Crosslinking reaction between PSSA-MA and PVA.

tra were measured on a Bruker FTIR spectrometer (Tensor 27) with Opus 7.0 measuring in the range of 4000–450 cm^{-1}. Thermogravimetric-differential thermal analysis (TGA-DTA) was carried out using Pyris Diamond TGA/DTA (PerkinElmer) system with a heating rate of 10 °C/min from 35–700 °C under nitrogen atmosphere. Glass transition temperature (T_g), melting temperature (T_m) and crystallization temperature (T_c) were obtained by differential scanning calorimetry (DSC) using a PerkinElmer Pyris 1 DSC. Samples were analysed with a heating rate of 10 °C/min from 50–250 °C under nitrogen flow.

Fibre preparation by electrospinning

Desired amounts of PSSA-MA, 9, 17, 25, 33, 42, and 50% by weight of PVA, were added to a 10 wt.% aqueous PVA solution. Imidazole was then added to the solution. The amount of imidazole used was fixed at 44% by weight of PSSA-MA to isolate the doping effect. The solutions were stirred overnight to ensure adequate mixing before electrospinning process prior to loading into a plastic syringe equipped with a 22-gauge stainless steel needle, connected to a high-voltage supply (DEL High-Voltage (0–100 kV), DEL Electronics Corp.). The polymer solutions were spun at a flow rate of 0.5 ml/h using a syringe pump (TERUMO Terufusion syringe pump TE-331, Japan). A piece of flat aluminium foil was placed 20 cm below the tip of the needle. The positive voltage applied was 19.4 kV. All experiments were performed at room temperature. The obtained fibres were later heated on a glass plate at 120 °C for 1 h to induce crosslinking reaction (Fig. 1) [24].

Membrane preparation

PSSA-MA (25% by weight of PVA) and imidazole (44% by weight of PSSA-MA) were added to a 10 wt.% PVA solution. The solution was stirred for 20 min prior to casting on a plastic plate, and drying at 80 °C for 18 h. The dried membrane was peeled off, and then heated on a glass plate at 120 °C for 1 h to induce crosslinking reaction.

Table 1 Electrospinning of PVA/PSSA-MA/imidazole solutions.

| PSSA-MA content (wt.%)	Observations
9	Fibre mat
17	Fibre mat
25	Fibre mat
33	Fibre mat
42	Solution droplets
50	Solution droplets

Proton conductivity

Proton conductivity measurements were made using impedance spectroscopy (Agilent E4980A Precision LCR Meter). The goal-coated membranes were placed between two electrodes followed by an application of 500 mV excitation voltage with a logarithmic frequency sweep from 1×10^2 Hz to 1×10^6 Hz. All measurements were conducted from 120–200 °C at 40 °C intervals. Resistance values were taken at the minimum imaginary response in a Z' versus Z'' plot to determine conductivity. The membrane conductivity was calculated from the membrane resistance, R, using $\sigma = l/RA$, where σ is the proton conductivity, l is the membrane thickness, and A is the cross-sectional area of the membrane sample.

RESULTS AND DISCUSSION

Electrospinning of polymer solutions

Electrospinning of solutions of PVA, PSSA-MA, and imidazole with various PSSA-MA contents, that is, 9, 17, 25, 33, 42, and 50%, was conducted at room temperature and constant electrospinning conditions (19.4 kV, 0.5 ml/h, 20 cm tip-to-target distance). Fibre mats were obtained from solutions with 9, 17, 25, and 33% PSSA-MA, while solution droplets were observed at higher PSSA-MA concentrations (Table 1). Solution properties play important roles in the synthesis of fibre via electrospinning. Fibre formation depends highly on viscosity, charge density, and surface tension[25–27]. Solution viscosities were plotted against PSSA-MA content (Fig. 2). It was found that solution viscosities increased with increasing PSSA-MA up to 33%. A drastic drop in viscosity at higher PSSA-MA concentrations, resulting from phase separation, is likely responsible for the non-spinnability of polymer solutions with 42 and 50% PSSA-MA.

SEM images of filers with 9–33% PSSA-MA show the increase in fibre size with increasing PSSA-MA (Fig. 3). The high viscosity results in a larger polymer jet and a consequent deposition of fibres with a larger diameter[28]. Only solution with
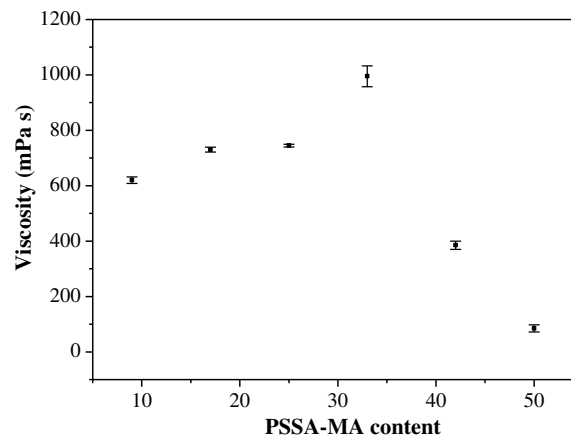
Fig. 2 Viscosities of polymer solutions as a function of PSSA-MA content.
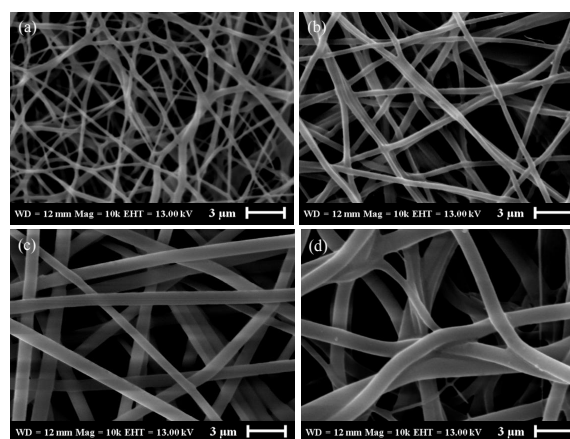
Fig. 3 SEM images (10 000× magnification) of electrospun fibres with various PSSA-MA contents. (a) 9, (b) 17, (c) 25, and (d) 33%.
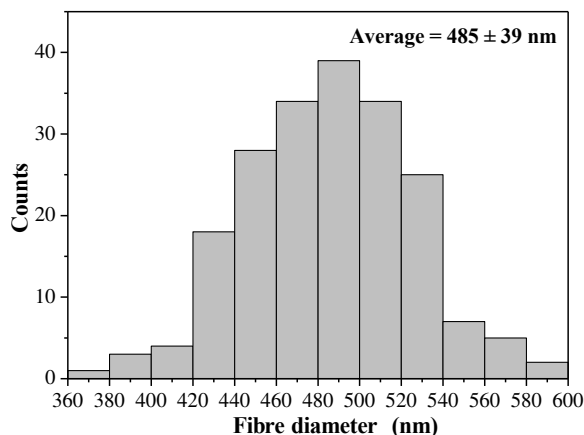
25% PSSA-MA provided uniform and untangled fibres with an average diameter of 485 ± 39 nm (Fig. 4). The thickness of the fibre mat was 0.32 mm.
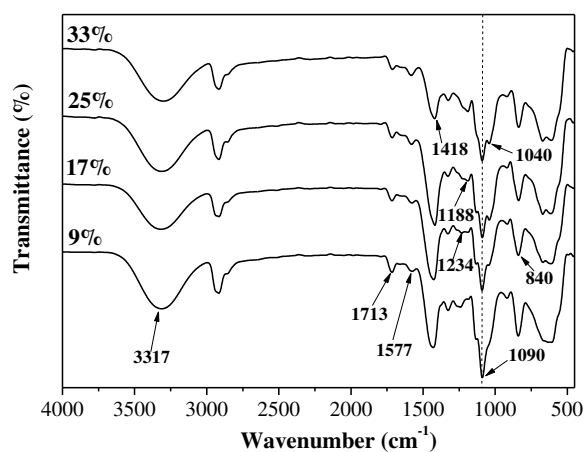
Membrane preparation

Proton conducting membrane containing 25% PSSA-MA was prepared from casting aqueous solution of PVA, PSSA-MA and imidazole on a plate. The membrane was allowed to dry at 80 °C prior to crosslinking reaction at 120 °C for 1 h. Free standing membrane with a thickness of 0.41 mm was obtained.

Fibre and membrane compositions

ATR-FTIR spectra of fibres comprising PVA, PSSA-MA and imidazole with four PSSA-MA concentrations after heat treatment were shown in
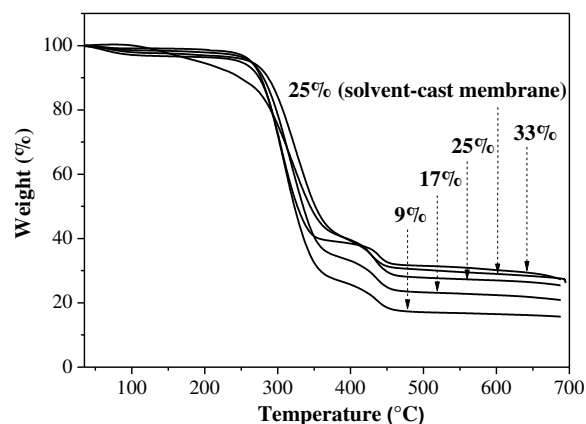
Fig. 4 Size distribution of electrospun fibres with 25% PSSA-MA.

Fig. 6 TGA thermograms of electrospun fibres with 9, 17, 25, and 33% PSSA-MA, and of solvent-cast membrane with 25% PSSA-MA.

intensity at 1090 cm^{-1} with increasing PSSA-MA concentration implied crosslinking reaction between PVA and PSSA-MA. Degree of crosslinking was found to increase as the wt.% of PSSA-MA increased. Similar peaks were observed for solvent-cast membrane with 25% PSSA-MA (data not shown).

Thermal properties

High thermal stability of membranes is required for good performances at elevated operating temperatures. TGA thermograms of heat-treated fibres were shown in Fig. 6. All samples were thermally stable up to approximately 250 °C, indicating sufficient thermal stability in the temperature range of proton conductivity measurements. Three main degradation stages were observed. The first weight loss below 140 °C could be attributed to the loss of absorbed water. The second loss between 140 and 380 °C was related to the losses of sulphonic acid pendants of PSSA-MA and PVA main and side chains. The third loss above 380 °C corresponded to the loss of PSSA-MA main chain[31–33]. A gradual increase in weight residue with increasing PSSA-MA suggested the increase in degree of crosslinking. Solvent-cast membrane with 25% PSSA-MA showed similar TGA thermogram to that of fibres.

Glass transition temperatures (T_g) and melting temperatures (T_m), obtained from DSC on the second heating cycle, of all fibres and membrane with 25% PSSA-MA were reported in Table 2. Crystallization temperature (T_c) on the first cooling cycle was also reported. All samples showed similar T_g values of approximately 81 °C. Slightly lower T_m and T_c values were observed for fibres, indicating the increase in

Fig. 5 FTIR spectra of heat-treated electrospun fibres with various PSSA-MA contents.

Fig. 5. The C−N stretching band of imidazole ring[29] was shown at 1577 cm^{-1}. The characteristic bands of PVA at 3317, 1418, and 1090 cm^{-1} could be designated to O−H stretching, O−H bending, and C−OH stretching, respectively[8]. Weak absorption bands corresponding to C=O of ester and C−O−C from polyvinyl acetate residue (5%) were also observed at 1713 and 1234 cm^{-1}, respectively. Absorption bands corresponding to PSSA-MA at 1188 and 1040 cm^{-1} were assigned to the S=O asymmetric and symmetric stretches, respectively[8]. The wagging vibration of C−H in 1,4-substituted benzene ring[30] of PSSA-MA was shown at 840 cm^{-1}. Although the increment in C−O−C peak intensity at 1234 cm^{-1} was not clearly observed due to the presence of relatively large amount of C−O−C linkage in pristine PVA, a decrease in C−OH peak

Table 2 DSC values of electrospun fibres and solvent-cast membrane with 25% PSSA-MA.

Sample	PSSA-MA (%)	T_g (°C)	T_m (°C)	T_c (°C)
Electrospun fibres	9	82.2	207.8	176.1
	17	81.9	209.1	177.8
	25	81.4	207.8	171.3
	33	82.7	210.7	176.3
Solvent-cast membrane	25	80.4	215.1	185.0
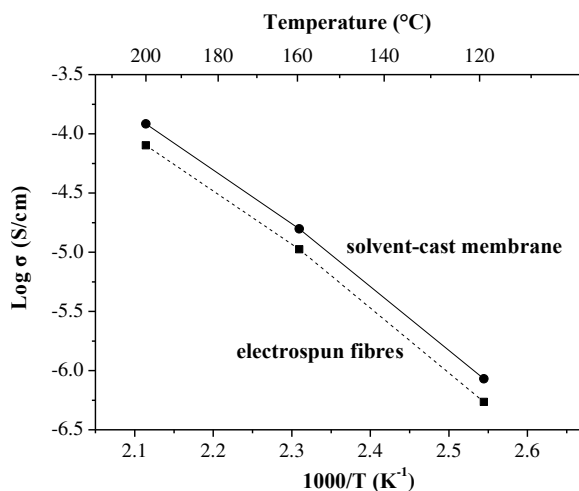
Fig. 7 Proton conductivities of electrospun fibres and solvent-cast membrane with 25% PSSA-MA.

interruption of the crystallization of PVA.

Proton conductivity

Proton conductivities of fibres and membrane with 25% PSSA-MA were determined from 120–200 °C on cooling down cycle in non-humidified condition. Fig. 7 showed the temperature dependence of proton conductivity as a function of reciprocal temperature. It was found that proton conductivity of solvent-cast membrane was slightly higher than that of fibres. In general, bulk conductivity is predominately governed by segmental mobility and charge carrier density[34]. A small difference in conductivities of fibrous membrane and solvent-cast membrane with similar T_g and identical charge carrier content suggests that there is at least one more factor that influences proton conductivity. Since the measurement of proton conductivity was conducted in the direction of membrane thickness, a denser membrane, that is solvent-cast membrane, might provide a more continuous hydrogen pathway for proton transport. A maximum conductivity of 121 µS/cm was achieved from solvent-cast membrane at 200 °C.

CONCLUSIONS

Proton conducting membranes based on crosslinked PVA, PSSA-MA, and imidazole for use at elevated temperatures were successfully prepared via electrospinning and solvent-cast methods. Fibre mats were obtained from most compositions; however, uniform fibres were only produced from solution with 25% PSSA-MA. Fibre diameter was found to increase with increasing solution viscosity. All membranes were thermally stable up to 250 °C under nitrogen atmosphere. The increase in PSSA-MA content resulted in an enhancement in thermal stability probably due to higher degree of crosslinking. Proton conductivity increased with increasing temperature. Besides mobility and charge carrier density in polymeric membranes, membrane density would likely be accounted for the small increment in conductivity of the solvent-cast membrane.

REFERENCES

1. Whittingham MS, Savinell RF, Zawodzinski T (2004) Introduction: Batteries and fuel cells. *Chem Rev* **104**, 4243–4.
2. Steele BCH, Heinzel A (2001) Materials for fuel-cell technologies. *Nature* **414**, 345–52.
3. Hickner MA, Ghassemi H, Kim YS, Einsla BR, McGrath JE (2004) Alternative polymer systems for proton exchange membranes (PEMs). *Chem Rev* **104**, 4587–611.
4. Küver A, Vielstich W (1998) Investigation of methanol crossover and single electrode performance during PEMDMFC operation: A study using a solid polymer electrolyte membrane fuel cell system. *J Power Sourc* **74**, 211–8.
5. Smitha B, Sridhar S, Khan AA (2006) Chitosan-poly(vinyl pyrrolidone) blends as membranes for direct methanol fuel cell applications. *J Power Sourc* **159**, 846–54.
6. Rhim JW, Yeom CK, Kim SW (1998) Modification of poly(vinyl alcohol) membranes using sulfur-succinic acid and its application to pervaporation separation

of water-alcohol mixtures. *J Appl Polymer Sci* **68**, 1717–23.

7. Chiang WY, Chen CL (1998) Separation of water-alcohol mixture by using polymer membranes—6. Water-alcohol pervaporation through terpolymer of PVA grafted with hydrazine reacted SMA. *Polymer* **39**, 2227–33.

8. Zhu M, He B, Shi W, Feng Y, Ding J, Li J, Zeng F (2010) Preparation and characterization of PSSA/PVA catalytic membrane for biodiesel production. *Fuel* **89**, 2299–304.

9. Gribov EN, Parkhomchuk EV, Krivobokov IM, Darr JA, Okunev AG (2007) Supercritical CO_2 assisted synthesis of highly selective nafion-zeolite nanocomposite membranes for direct methanol fuel cells. *J Membr Sci* **297**, 1–4.

10. Silva VS, Ruffmann B, Silva H, Silva VB, Mendes A, Madeira LM, Nunes S (2006) Zirconium oxide hybrid membranes for direct methanol fuel cells—Evaluation of transport properties. *J Membr Sci* **284**, 137–44.

11. Rikukawa M, Sanui K (2000) Proton-conducting polymer electrolyte membranes based on hydrocarbon polymers. *Progr Polymer Sci* **25**, 1463–502.

12. Smitha B, Sridhar S, Khan AA (2005) Solid polymer electrolyte membranes for fuel cell applications—a review. *J Membr Sci* **259**, 10–26.

13. Zhang JL, Xie Z, Zhang JJ, Tanga YH, Song CJ, Navessin T, Shi ZQ, Song DT, Wang HJ, Wilkinson DP, Liu ZS, Holdcroft S (2006) High temperature PEM fuel cells. *J Power Sourc* **160**, 872–91.

14. Shao YY, Yin GP, Wang ZB, Gao YZ (2007) Proton exchange membrane fuel cell from low temperature to high temperature: Material challenges. *J Power Sourc* **167**, 235–42.

15. Li QF, He RH, Jensen JO, Bjerrum NJ (2003) Approaches and recent development of polymer electrolyte membranes for fuel cells operating above 100 °C. *Chem Mater* **15**, 4896–915.

16. Kreuer KD, Paddison SJ, Spohr E, Schuster M (2004) Transport in proton conductors for fuel-cell applications: Simulations, elementary reactions, and phenomenology. *Chem Rev* **104**, 4637–78.

17. Münch W, Kreuer KD, Silvestri W, Maier J, Seifert G (2001) The diffusion mechanism of an excess proton in imidazole molecule chains: first results of an ab initio molecular dynamics study. *Solid State Ionics* **145**, 437–43.

18. Schuster MFH, Meyer WH (2003) Anhydrous proton-conducting polymers. *Annu Rev Mater Res* **33**, 233–61.

19. Borup R, Meyers J, Pivovar B, Kim YS, Mukundan R, Garland N, Myers D, Wilson M, et al (2007) Scientific aspects of polymer electrolyte fuel cell durability and degradation. *Chem Rev* **107**, 3904–51.

20. Tamura T, Kawakami H (2010) Aligned electrospun nanofiber composite membranes for fuel cell electrolytes. *Nano Lett* **10**, 1324–8.

21. Chen H, Snyder JD, Elabd YA (2008) Electrospinning

and solution properties of nafion and poly(acrylic acid). *Macromolecules* **41**, 128–35.

22. Bajon R, Balaji S, Guo SM (2009) Electrospun nafion nanofiber for proton exchange membrane fuel cell application. *J Fuel Cell Sci Tech* **6**, 0310041–6.

23. Martwiset S, Jaroensuk K (2012) Electrospinning of poly(vinyl alcohol) and poly(4-styrenesulfonic acid) for fuel cell applications. *J Appl Polymer Sci* **124**, 2594–600.

24. Kim DS, Park HB, Rhim JW, Lee YM (2005) Proton conductivity and methanol transport behavior of cross-linked PVA/PAA/silica hybrid membranes. *Solid State Ionics* **176**, 117–26.

25. Huang ZM, Zhang YZ, Kotaki M, Ramakrishna S (2003) A review on polymer nanofibers by electrospinning and their applications in nanocomposites. *Compos Sci Tech* **63**, 2223–53.

26. Greiner A, Wendorff JH (2007) Electrospinning: A fascinating method for the preparation of ultrathin fibers. *Angew Chem Int Ed* **46**, 5670–703.

27. Schiffman JD, Schauer CL (2008) A review: Electrospinning of biopolymer nanofibers and their applications. *Polymer Rev* **48**, 317–52.

28. Zhong Z, Cao Q, Wang XY, Wu N, Wang Y (2012) PVC-PMMA composite electrospun membranes as polymer electrolytes for polymer lithium-ion batteries. *Ionics* **18**, 47–53.

29. Boroglu MS, Celik SU, Bozkurt A, Boz I (2011) The synthesis and characterization of anhydrous proton conducting membranes based on sulfonated poly(vinyl alcohol) and imidazol. *J Membr Sci* **375**, 157–64.

30. Bekri-Abbes I, Bayoudh S, Baklouti M (2006) Converting waste polystyrene into adsorbent: Potential use in the removal of lead and cadmium ions from aqueous solution. *J Polymer Environ* **14**, 249–56.

31. Martwiset S, Woudenberg RC, Granados-Focil S, Yavuzcetin O, Tuominen MT, Coughlin EB (2007) Intrinsically conducting polymers and copolymers containing triazole moieties. *Solid State Ionics* **178**, 1398–403.

32. Cho CG, Jang HY, You YG, Li GH, An SG (2006) Preparation of poly(phenylene oxide-g-styrenesulfonic acid) and their characterization for DMFC membrane. *High Perform Polymer* **18**, 579–91.

33. Holland BJ, Hay JN (2001) The thermal degradation of poly(vinyl alcohol). *Polymer* **42**, 6775–83.

34. Persson JC, Jannasch P (2003) Self-conducting benzimidazole oligomers for proton transport. *Chem Mater* **15**, 3044–5.